Detection of Domestication Signals through the Analysis of the Full Distribution of Fitness Effects using Simulations

Ioanna-Theoni Vourlaki[1†], David Castellano[2†], Ryan N. Gutenkunst[2*], Sebastian E. Ramos-Onsins[1*]

1. Centre for Research in Agricultural Genomics (CRAG), Autonomous University of Barcelona (UAB), Vall de la Moronta s/n, Cerdanyola del Valles, Barcelona, 08193, Spain.

2. Department of Molecular and Cellular Biology, University of Arizona, Tucson, AZ, USA.

† Equal contribution

*Co-corresponding authors

ABSTRACT

The process of domestication involves a complex interplay between concurrent demographic and selective changes. While we can readily observe the phenotypic effects of domestication, the genetic consequences of domestication often remain elusive. Artificial selection can alter the selection coefficients of both new and pre-existing genetic variation within domesticated populations. To investigate this, we conducted simulations using a combination of population genomic parameters designed to reflect the domestication process observed in large livestock mammals. Our study uses forward-in-time simulations to examine the 1D and 2D site frequency spectra (SFS) of mutations in two populations that have diverged since the domestication split. In total, we examined eighteen different scenarios, varying the strength of selection acting on beneficial mutations and the proportion of mutations with altered selection coefficients post-domestication. First, we discuss how linked selection and fluctuating selection coefficients affect the accuracy of inferred demographic histories. Second, we find that certain aspects of the full distribution of fitness effects (DFE), such as the shape and strength of the deleterious DFE, can be accurately estimated in both populations using only the 1D-SFS. However, the accurate characterization of the beneficial DFE remains a challenge, even when using the 2D-SFS. Third, using a novel joint DFE model, we are able to quantify the fraction of mutations that have experienced a change in their selection coefficient (p_C) during domestication. Interestingly, classic hard selective sweeps can mimic a substantial increase in p_C, even when the simulated p_C was initially zero. In summary, our work highlights the strengths and limitations of detecting changes in the DFE, and emphasizes the risks of over-interpreting demographic histories across a range of realistic domestication scenarios.

Keywords: Domestication, DFE, demography, selective sweeps, linked selection, 2D-SFS, forward-in-time simulations.

INTRODUCTION

The increase in human population and the emergence of modern society are linked to the domestication of plants and animals (Purugganan and Fuller 2009; Driscoll *et al.* 2009; Larson and Burger 2013; Amills *et al.* 2017). Human civilization it was made possible by the domestication of surrounding life forms, where humans began to domesticate plants and animals such as wheat, dogs, pigs, or chickens (Dayan 1994; Zeder *et al.* 2006; Zeder 2012, 2015; Redding 2015; Avni *et al.* 2017). Domestication is a process that allows humans and other species to establish a long-term mutualistic relationship that provides benefits to both species (Zeder *et al.* 2006). Human domestication of fauna and flora began about 10-15 thousand years ago and is still ongoing (Larson and Burger 2013; Zeder 2015). Although human civilization is based on domestication, we still lack a complete genomic and evolutionary understanding of domestication. Domestication is a rapid process on the evolutionary time scale, but it is not a discrete event and implies the gradual improvement of domesticated traits. It is believed that human-induced artificial selection during domestication can be expected to be relatively stronger and therefore faster than natural selection. However, in plants it has been shown that the evolutionary rate of domesticated varieties is similar to that of wild plants, suggesting a process similar to natural selection (Purugannan and Fuller 2010). In addition, domestication tends to be associated with bottlenecks; only a small number of individuals from the wild population are domesticated, which is expected to reduce the efficiency of natural selection (Wright *et al.* 2005). Another important difference between natural and artificial selection is that modern breeders typically use truncation selection, which is the selection of the top percentage of individuals for the desired trait (Granleese *et al.* 2019). The prevalence of truncation selection in nature, or prior to industrialization, is unknown. Truncation selection is known to be a simple and efficient form of directional selection (Crow and Kimura 1979), and no severe accumulation of genetic load is expected in outcrossing species (Kondrashov 1988; Ohta 1989) if the population size remains large enough (Marsden *et al.* 2016). A recent comprehensive meta-analysis of the genetic costs of domestication (Moyers *et al.* 2018) found that deleterious variants are more numerous (or segregate at higher frequencies) in domesticated populations compared to their wild relatives However, this pattern may not be general, as seen in sorghum (Lozano et al. 2021). This pattern is likely driven by a number of processes that collectively reduce the effectiveness of selection in domesticated populations, as first suggested in rice genomes (Lu *et al.* 2006).

Selection, both natural and artificial, can occur through either a few loci with strong effects or many loci with small effects (Jain and Stephan 2017a; b), depending on the genetic architecture of the trait and the strength of selection on it. Different patterns of genetic diversity around selected loci are expected in response to these two models of selection (Stephan and John 2020). Classic hard selective sweeps have been reported at a few candidate loci among important domesticated traits (Andersson 2012), such as the IGF2 gene region associated with lean domestic pigs (Van Laere *et al.* 2003), the thyroid-stimulating hormone receptor (TSHR) in domestic chickens (Rubin *et al.* 2010), or the sh4 and qSW5 loci (Shomura *et al.* 2008; Li *et al.* 2018) involved in the traits of seed shattering and grain width, respectively, in domestic rice (Huang *et al.* 2012). These examples are consistent with a simple Mendelian genetic architecture, in which a few loci account for most of the variance in the domesticated trait (for a comprehensive list of genes important for domestication, see Courtier-Orgogozo and Martin 2020).

Polygenic adaptation, on the other hand, describes a process in which a constellation of small changes in allele frequencies modify differences in the trait under selection, where a trait is a phenotypic trait but also can be the fitness itself. A wide range of population genetic models and simulations have been examined to describe polygenic adaptation (de Vladar and Barton 2014; Stephan 2016). Some models analyze the polygenic response of a trait in the presence of mutation and stabilizing selection (de Vladar and Barton 2014; Stephan and John 2020), while others capture the response of a trait under mutation and stabilizing or directional selection following an environmental change in a finite size population (Jain and Stephan 2017a; Devi and Jain 2023). In practice, polygenic adaptation using genetic data is harder to detect than classic selective sweeps (Pritchard et al. 2010), but the combined use of phenotypic data together with genetic data can detect the selective effect of quantitative traits (e.g., Chen et al. 2021, Berg and Coop 2014). Polygenic adaptation has been detected in some specific studies in wild, domesticated and experimental evolution populations (Barghi *et al.* 2019; Reid *et al.* 2023; He *et al.* 2023).

In this study, we ask to what extent we can detect a genomic signal of domestication using a different approach: comparing the full distribution of fitness effects (DFE) on new and standing variation. To do this, we inferred the full DFE of new non-synonymous mutations in wild and domesticated populations. The DFE of new deleterious mutations has previously been estimated by contrasting the 1D-SFS of synonymous and non-synonymous mutations from a

variety of species, assuming that beneficial mutations contribute only to divergence but not to polymorphism due to their rapid fixation in the population (Keightley and Eyre-Walker 2007; Boyko *et al.* 2009; Kim *et al.* 2017; Tataru *et al.* 2017; Barton and Zeng 2018). Tataru *et al.* (2017) proposed a model, polyDFE, to infer the full DFE and the proportion of adaptive substitutions (α) using only polymorphism data. Castellano *et al.* (2019) used polyDFE to compare the full DFE of new amino acid mutations across great apes, and found that the shape of the deleterious DFE is constant across this set of closely related species. More recently, a new method using 2D-SFS has been proposed to jointly estimate the full DFE between two populations that recently diverged and share many polymorphisms (Huang *et al.* 2021).

However, few studies have compared the DFE between domesticated and wild populations (Leno-Colorado *et al.* 2022). First, the analysis of differences between wild and domesticated individuals has been focused on finding large effects that determine the phenotypic differences between these two groups. Therefore, DFE does not appear to be an adequate method for detecting candidate regions, as DFE considers the entire distribution of selective effects and appears to be blind to single events. Second, the split between wild and domestic populations is very recent (expected to be no more than 10K years), suggesting that the DFE of these two populations would be very similar or identical. Third, methods to detect subtle differences in DFE between two closely related populations have not been developed.

On the other hand, the study of the demographic processes involved in domestication has been addressed in several species (e.g., Miranda et al. 2023, Arnoux et al. 2020, Murray et al. 2010), where the split between wild and domestic populations, bottlenecks, and gene flow events between these two populations have been inferred, also considering multiple selective sweeps (Caicedo et al. 2007). It has also been shown (Torres et al. 2020) that ignoring deleterious selective effects in the study of demographic patterns, can lead to biased estimates of silent variability patterns (see also Comeron 2017, Beissinger et al 2016). Thus, it is suggested that the DFE and demography be inferred together to avoid deviations from the true value.

Here, we use forward-in-time simulations that consider the domestication process under different demographic and selective models. Several combinations of genetic architectures and selective effects have been simulated, ranging from one that considers a relatively small number of loci that change their selective effects to another that considers polygenic adaptation (considering fitness as a trait) where many loci have divergent selective effects. In all cases,

131 the selective effects of a fraction of the existing variants can change (from deleterious to
132 beneficial and vice versa) in the domesticated population. We also describe how linked
133 selection and changing the DFE deform the recovered demographic histories.

134

MATERIALS AND METHODS

Simulation of the Domestication Process

A simulation analysis of the domestication process is developed using the forward-in-time simulator SLiM4 (Haller and Messer 2023). The general model of the domestication process is developed in the SLiM script available in github (https://github.com/CastellanoED/domesticationDFE). Eighteen different domestication scenarios are analyzed, and the parameters for each scenario are shown in Table 1. All options (flags) used to run the SLiM script are also available in github (https://github.com/CastellanoED/domesticationDFE). We aim to model a general domestication process that resembles the genomic configuration, generation time, mutation and recombination landscape relevant to large domesticated mammals used as livestock. The constructed model assumes a genome containing a single chromosomal "chunk" or window, with 10,000 loci/exons of 120 base pairs in length, and each locus/exon with one-third (4-fold) neutral synonymous positions and two-thirds (0-fold) selected non-synonymous positions scattered along the locus.

The simulation parameters for each scenario (Figure 1A) are as follows: the initial ~~blank~~ population at time 0 run for 10*N_e generations to reach mutation-selection-drift equilibrium, then splits into the domesticated and wild populations. Hereafter we refer to the Wild and Domestic populations. We aim to mimic a realistic but still general domestication process in large livestock mammals where ancestral N_e estimates are on average around 10,000 (Murray *et al.* 2010; Groenen *et al.* 2012; Larson *et al.* 2014; Frantz *et al.* 2015; Yang *et al.* 2016; Librado *et al.* 2021; Todd *et al.* 2022) and the domestication process, according to archeological records, started around 10,000 years ago (Ahmad *et al.* 2020). The average generation time in these large domestic mammals is about 5 years per generation (Pacifici *et al.* 2013). Note that in this study we had to reduce the population size and related population parameters below from 10,000 diploid individuals to N_e=5,000 diploid individuals for computational reasons.

Genomic parameters: The mutation rate per site (μ) and generation is $2.5\text{x}10^{-7}$, and the population size (N_e) is 5,000 diploid individuals, thus the expected θ under neutrality is **0.005**. Each locus is separated from its neighbors by $3\text{x}10^{-6}$ recombination events per generation. The

recombination rate per site and generation within the loci is fixed to a rate of $1.5x10^{-7}$ recombination events per site. Note that the higher recombination between loci aims to mimic their real genetic distance separation (assuming a functional site density of 5%) - this greatly speeds up the simulation as non-coding sites do not need to be simulated. In other words, we simulate 120 Kb of coding sequence in each run, which is equivalent to simulating a 2.4 Mb chromosome window with 5% coding sites. We perform 100 independent runs for each of the eighteen scenarios.

Demographic parameters: The Domestic populations of 5,000 diploid individuals suffer a bottleneck, reducing their population size temporarily to 200 diploid individuals, to recover again to 5,000 diploid individuals after the bottleneck. The bottleneck lasted 100 generations. The simulation finishes 900 generations after the bottleneck. In nine of the eighteen simulated scenarios we allow that 1% of the Wild individuals migrate to the Domestic population during the 100 generations of the bottleneck. Thus, during the bottleneck 25% of the domesticated population is wild. In the other nine combinations there is no exchange of individuals between the Wild and Domestic populations. This demographic history is equivalent to a 1,000 years long bottleneck followed by a 9,000 years long recovery in an ancestral population with 10,000 diploid individuals and a generation time of 5 years.

DFE parameters: The selective effects produced by domestication are modeled by changing the fitness values of a proportion of the existing and new mutations in the domestic population (at the time of the split) (Table 1). We call this probability of change p_c and it can be 0% (our negative control), 5% or 25%. Domesticated and Wild populations show different proportions of beneficial and deleterious new mutations depending on the scenario. The negative effects in all scenarios and populations follow a gamma distribution with a shape value of 0.3 and a mean of S_d = -100 ($2N_es_d$ in the heterozygote, N_e = 5,000 diploid individuals and s_d = -1%), which is in the range of values inferred using empirical data (Boyko et al. PLoS Genet 2008, Galtier PLoS Genet 2016), while variants with positive effects follow an exponential distribution. We investigate three combinations of parameters for the positive DFE: pervasive & nearly neutral (with mean selective effects S_b of 1 and probability of being beneficial p_b of 10%), common & weak (S_b = 10 and p_b = 1%) and rare & strong (S_b = 100 and p_b = 0.1%) (Table 1).

Types of Sites

The sites are initially divided into seven different types (named m_1 to m_7), being m_1 neutral (synonymous) and m_2 to m_7 functional (non-synonymous) sites having a different selective effect when mutated (see Table 2 and Figure 1C). Mutations at m_5, m_6 and m_7 sites generate deleterious variants in the Wild population, and mutations at m_2, m_3 and m_4 sites generate beneficial mutations in the Wild population. The selection coefficient of mutations generated at m_2 (beneficial) or at m_5 (deleterious) sites are invariant for the Wild and Domestic populations. However, the mutations at m_3, m_4, m_6 and m_7 sites will change their selective effect in the Domestic populations relative to the Wild populations. That is, the new selective effect is drawn from the corresponding DFE section (positive or negative), independently of their value in the wild population. ~~Those can be understood as sites with divergent selective effects.~~ The selection coefficient of a given beneficial mutation at m_3 sites will remain beneficial in the Domestic population, but it will be different from the original beneficial effect at Wild. A mutation at m_4 sites will change its selection coefficient from beneficial in the Wild to deleterious in the Domestic population. Equivalently, the selection coefficient of a deleterious mutation at m_6 sites will remain negative in the Domestic population but it will be different from that found at Wild. A mutation at m_7 sites will change its selection coefficient from deleterious in the Wild to beneficial in the Domestic population. For each of the 18x100 independent simulation runs, we randomly precalculate the location of each site type (except for the permanent disposition of two non-synonymous sites followed by a synonymous site within codons) using

an ad hoc R script. This hard-coding of selective effects on different sites allows us to gain insight into the relative importance of each mutation type for the domestication process.

Distribution of fitness effects (DFE): Two complementary approaches

polyDFE: 1D-SFS and 1D-DFE

We use the polyDFEv2.0 framework (Tataru and Bataillon 2019) to estimate and compare the DFE across Wild-Domestic population pairs by means of likelihood ratio tests (LRTs). We use the R function compareModels (from https://github.com/paula-tataru/polyDFE/blob/master/postprocessing.R) to compare pairs of models. The inference is performed only on the unfolded SFS data (divergence counts to the outgroup are not fitted), and unfolded SFS data are fitted using a DFE model comprising both deleterious (gamma

distributed) and beneficial (exponentially distributed) mutations. The DFE of each Wild-Domestic population pair is inferred using the 1D-SFS of each population. polyDFE assumes that new mutations in a genomic region arise as a Poisson process with an intensity that is proportional to the length of the region and the mutation rate per nucleotide (μ). We assume that μ remains constant across simulations (as it is the case). Both an ancestral SNP misidentification error (ε) and distortion parameters (r_i) are estimated. However, we notice that the exclusion of ε does not affect the rest of estimated parameters because under the simulation conditions used here no sites are expected to be misidentified. The r_i parameters are fitted independently for each frequency bin (from n = 1 to n = 19), and they are able to correct any distortion that affects equally the SFS of synonymous and non-synonymous variants (such as, in principle, demography or linked selection). Model averaging provides a way to obtain honest estimates that account for model uncertainty. To produce the model average estimates of the full DFE we weight each competing model according to their AIC following the equation 6.1 shown in the polyDFEv2 tutorial ("polyDFE/tutorial.pdf at master · paula-tataru/polyDFE"). We use the R function getAICweights (from https://github.com/paula-tataru/polyDFE/blob/master/postprocessing.R to do the model averaging R) to obtain the AIC values.

dadi: 2D-SFS and 2D-DFE

dadi (Gutenkunst *et al.* 2009) is employed to infer the joint distribution of fitness effects (Jerison *et al.* 2014; Ragsdale *et al.* 2016; Huang *et al.* 2021) and the demographic history of all simulated population pairs. Our new model for the joint DFE between the two populations is a mixture of multiple components designed to mimic the selected mutation types in the simulations (Table 2; Figure 1D). The major exception is that beneficial mutations are modelled to have a single fixed selection coefficient, rather than arising from an exponential distribution. Let p_{+W} be the fraction of mutations that are positively selected in the Wild population, p_C be the fraction of mutations that change selection coefficient in the Domestic population, and p_{C+} be the fraction of those mutations that become beneficial in the Domestic population (note in our simulations $p_{+W} = p_{C+}$). To model mutation types m2 and m3, a proportion p_{+W} x (1-p_C) + p_{+W} x p_C x p_{C+} of mutations are assumed to have the same fixed positive selection coefficient in both populations. To model m4, a proportion p_{+W} x p_C x (1-p_{C+}) is assumed to have a fixed positive selection coefficient in the Wild population and a

gamma-distributed negative selection coefficient in the Domestic population. To model m5, a proportion (1-p_{+w}) x (1-p_c) of mutations are assumed to have equal negative gamma-distributed selection coefficients in the two populations. To model m6, a proportion (1-p_{+w}) x p_c x (1-p_{c+}) is assumed to have independent gamma-distributed selection coefficients in the two populations. To model m7, a proportion (1-p_{+w}) x p_c x p_{c+} mutations is assumed to have a gamma-distributed negative selection coefficient in the Wild population and a fixed positive selection coefficient in the Domestic population. All gamma distributions are assumed to have the same shape and scale. This model is implemented in *dadi* as the function **dadi.DFE.Vourlaki_mixture**. Note in our simulations the marginal 1D-DFEs of Wild and Domesticated populations are exactly the same; the difference is that in Domesticated populations a given fraction of sites (some already polymorphic, some still monomorphic) can change their selection coefficient relative to the Wild population.

For inference, a new, more general demographic model with branch-independent population size changes is first fit to the synonymous mutations from each simulation, and then the newly proposed joint DFE model is fit to the non-synonymous mutations. The parameters of the demographic model (Figure 1B) are estimated by running 100 optimizations per inference unit. The 2D-SFS for selected sites are precomputed conditional on the demography for 104^2 values of γ_1 and γ_2 ($2N_as$, a population scaled selection coefficient for the heterozygote where N_a is the ancestral population size), 102 negative and 2 positives. For the negative part of the DFE, γ values were logarithmically equally spaced between -2000 and -10^{-4}. The expected DFE for selected sites can then be computed as a weighted sum over these cached spectra (Kim *et al.* 2017). The DFE parameters shape, scale, p_{+w}, p_c, and p_{c+} are then estimated by maximising the Poisson likelihood of the simulated data, with the non-synonymous rate of mutation influx fixed to twice that inferred for neutral sites in the demographic history fit. For the DFE inference, optimization is repeated until the best three results are within 0.5 log-likelihood units. Ancestral state misidentification is modelled, however in our simulations no sites are expected to be misidentified.

For the purpose of this work, *dadi* software is downloaded and installed according to the instructions provided at the following link: https://bitbucket.org/gutenkunstlab/dadi/src/master/. Since *dadi* operates as a module of

287 Python, the Anaconda3 and Spyder (Python 3.7, Rossum and Drake 2009; Anaconda 2016;
288 Raybaut 2009) versions are used in this study.

289 **Inference units, and confidence intervals in demographic and DFE parameters**

290 To obtain the sampling variance of parameter estimates and approximate confidence intervals,
291 we use a bootstrap approach. We resample with replacement 100 times 20 independent
292 simulation runs or chromosomal "chunks" (from a pool of 100 "chunks") and concatenate
293 them. Hence, each concatenated unit (or inference unit) is made of 24 Mb of coding sequence
294 (as comparison, the human genome contains ~26 Mb of coding sequence). Uncertainties of
295 DFE parameter inferences in polyDFE and *dadi* are calculated by this conventional
296 bootstrapping, but in *dadi* we hold the demographic model fixed. In polyDFE the distortion
297 introduced by demography (and linked selection) is not estimated but corrected with the r_i
298 parameters. Note that our procedure with *dadi* does not propagate uncertainty in demographic
299 parameters through to the DFE parameters. To obtain the sampling variance of demographic
300 parameter estimates with *dadi* we use the Godambe approach as described in Coffman *et al.*
301 2016. A final consideration on the factor of two differences across simulation and inference
302 tools. In polyDFE, s is defined as the selection coefficient on the heterozygote (as in *dadi*), and
303 the scaled selection coefficient is defined as $4N_e s$, while in *dadi* it is defined as $2N_a s$ (in the
304 ancestral population). In SLiM2, s is defined as the selection coefficient on the homozygote.

305

306 **RESULTS AND DISCUSSION**

307 Studying the effect of domestication on the DFE of natural populations can be very challenging,
308 especially when available methods for inferring and comparing the DFE have not been
309 compared using exactly the same dataset. In the present work, we conduct a simulation study
310 using different combinations of parameters relevant to the domestication process. Note that the
311 main difference between domestication demographic model used here and demographic
312 models used in speciation studies is the time scale since the split occurred. Our simulated
313 domesticated populations experience a large or small change in the number and selective
314 effects of loci under domestication after a bottleneck period, with or without migration.
315 Hereafter, we refer to the Wild and Domestic populations.

316 The Wild populations have a constant DFE and constant population size, but limited
317 recombination across loci to mimic a realistic recombination landscape. Beneficial mutations
318 arise at Wild populations following an exponential distribution, while deleterious mutations
319 are drawn from a gamma distribution with shape 0.3 and mean S_d = -100 (where $S_d = 2N_a s_d$,
320 the selection coefficient s_d in the heterozygote is -1%, and N_a = 5,000 diploid individuals is
321 the ancestral effective population size, see Material and Methods: Simulating the
322 Domestication Process). All mutations, beneficial and deleterious, are co-dominant. The
323 Domestic population originates from the Wild population through a bottleneck and a
324 concomitant change in selective effects at a fraction of non-synonymous sites (Figure 1; Table
325 1). The recombination and mutation landscapes are drawn from the same distribution in the
326 Domestic and Wild populations.

327 The change in selective effects affects both new mutations that arise within the Domestic
328 population and existing variants that existed before the domestication event. Put simply, not
329 only can mutations that were deleterious (or beneficial) before the population split become
330 beneficial (or deleterious) within the domestic population, but even if the direction of the
331 selective effect remains the same, the intensity of selection can change. Table 2 shows all the
332 combinations of changes in selective effects between Wild and Domestic populations. Our
333 simulated scenarios aim to cover a variety of possible changes in the genetic architecture
334 (number of loci) and the strength of selection (selection coefficients) of the trait/s under
335 domestication. Three DFEs for beneficial mutations are assumed: (i) pervasive and nearly
336 neutral, where a large fraction of new mutations (10%) are on average nearly neutral (S_b = 1),

337 (ii) common and weak, where beneficial mutations are still fairly common (1%) but weakly
338 selected (S_b = 10) and (iii) rare and strong, where very few mutations (0.1%) are strongly
339 beneficial (S_b = 100). Depending on the scenario, a selective change occurs only at a small
340 (5%) or at a substantial proportion (25%) of sites in the Domestic population (Table 1, "p_c"
341 column). We leave six scenarios as negative controls; the selection coefficients of new and
342 standing variation in the Domestic and Wild populations are exactly the same. Finally,
343 demographic changes affect only the Domestic population; the Wild population evolves under
344 a constant population size. Two versions of the same demographic model (Figure 1A) are
345 simulated: (i) one with migration, and (ii) another without migration. When there is migration,
346 it only occurs from the Wild to the Domestic population during the domestication bottleneck.

347 **Estimation of demographic parameters in Wild and Domestic populations**

348 In this study, we investigate the effects of natural selection, both in a general sense and
349 specifically the change in selection coefficient in shared variation due to artificial selection, on
350 our ability to reconstruct the demographic history of domestication and the DFE. We do this
351 using two commonly used inference tools (polyDFE and *dadi*) that assume free recombination
352 across loci. Note that *dadi* first infers the demographic history and then infers the DFE
353 assuming those inferred demographic parameters, whereas polyDFE operates independently of
354 specific demographic histories and is designed to correct for distortions that affect both
355 synonymous and non-synonymous site frequency spectra equally (Tataru and Bataillon 2019).
356 Figure 1 A and B show the simulated joint demographic model and the joint demographic
357 model used in the *dadi* inferences, respectively. We have increased
358 the complexity of the inference model by introducing additional parameters, allowing it to
359 account not only for "simulated" or true demographic changes, but also for more complex and
360 unknown demographic histories and the potential influence of linked selection on synonymous
361 SFS. The diagnostic plots can be found in Supplementary Figure 1; there is good agreement
362 between the model fits and the data.

363 Our findings indicate that when positive selection is relatively weak (S_b = 1 or S_b = 10), the
364 estimated onset of domestication tends to be approximately twice as old as the actual simulated
365 starting point. Additionally, the bottleneck appears slightly shallower but considerably longer
366 than the simulated value (see Figure 2 and Supplementary Table 1 for the confidence intervals).
367 This suggests that the influence of linked selection, likely driven primarily by background

368 selection when S_b <= 10, has the effect of elongating the timeline. Consequently, it makes the
369 domestication divergence and bottleneck appear more ancient and extended, respectively. For
370 the Wild populations we always detect a larger population expansion than for the Domestic
371 populations, but without a bottleneck. This signal of a recent expansion in the Wild population
372 is expected because when we consider how linked selection affects the SFS, there are more
373 rare synonymous polymorphisms compared to what we would expect if there was free
374 recombination under a constant population size (Nielsen 2005). Remarkably, when positive
375 selection is strong (S_b = 100), the temporal stretch becomes even more pronounced and the
376 demographic history of both populations overlap extensively. The domestication divergence
377 shifts to approximately 50,000 years ago, whereas the actual simulated split occurred 10,000
378 years ago. Additionally, the bottleneck appears significantly longer and less severe, while there
379 is an inferred large population expansion in both Wild and Domestic populations. Although in
380 Figure 2 there appears to be a change in population size before the domestication split, only
381 three scenarios (with IDs 5, 6, and 7) are statistically significant (Supplementary Table 1 and
382 Supplementary Figure 2). Interestingly, we find the migration rate from Wild to Domestic
383 (m_{w2d}) and from Domestic to Wild (m_{d2w}) are overestimated in all scenarios (Supplementary
384 Table 1 and Supplementary Figure 3). We observe that neither migration nor an increase in p_c
385 appears to significantly change the inferred demographic histories that we have just described.

386 Torres et al. (2020) detected a distortion in the patterns of diversity due to deleterious effects.
387 Instead, we detected a distortion in the demographic inference that differs depending on
388 positive selective effects. Our findings indicate that when linked selection is at play, the
389 reconstructed demographic history captures certain elements of the actual simulated history.
390 For instance, if positive selection is not strong, it successfully identifies a bottleneck in
391 Domestic populations compared to Wild populations. However, when positive selection is
392 strong (S_b = 100), it tends to "erase" the demographic history through indirect selection effects
393 and recreate large recent population expansions in both populations. Nevertheless, and more
394 importantly, in all scenarios it is not possible to accurately determine the timing of the onset of
395 domestication, the duration of the domestication bottleneck, or to distinguish between the
396 presence and absence of migration between populations. We believe that these aspects are
397 crucial for contextualizing the role of domestication in human history. Unfortunately, either
398 the 2D-SFS or our modeling assumptions (or both) do not seem to be useful in this context.

399 Thus, the next question is to what extent can the nuisance r_i parameters from polyDFE or this
400 distorted inferred demography from *dadi* help to recover the simulated DFE parameters?

401 **Can domestication be detected as an artificial change in the marginal full DFE**
402 **between populations? No.**

403 Next, we investigate whether polyDFE captures differences in the marginal (or 1D) full DFE
404 of Domestic and Wild populations across the eighteen domestication scenarios (Table 1). We
405 run five nested models (Table 3) and compare them using likelihood ratio tests (LRTs)
406 (Supplementary Table 2). It is important to note that in all our simulations, the marginal full
407 DFE for new mutations in both Domestic and Wild populations is the same within a given
408 scenario (as detailed in Table 1). This means that the selection coefficients for sites, whether
409 they are monomorphic or polymorphic, are drawn from the same full DFE. In simpler terms,
410 the proportion of new mutations that are advantageous or detrimental is identical for both
411 Domestic and Wild populations within a given scenario. The key distinction lies in the fact that
412 when $p_C > 0\%$, Domestic populations might have a higher number of advantageous mutations
413 as polymorphisms. This is because some of these beneficial mutations were already present at
414 intermediate or high frequencies as nearly neutral polymorphisms in the ancestral population,
415 and we expect that migration after the domestication split can also re-introduce beneficial
416 mutations from the Wild to the Domestic population.

417 LRTs between different nested models allow us to address important questions about
418 the DFE, without assuming any prior knowledge of our datasets. First, we assess whether the
419 inferred shape of the negative DFE is similar in both populations while also examining if the
420 estimation of the shape parameter is influenced by the presence of advantageous mutations.
421 When comparing models that do not consider beneficial mutations (models M1 versus M10
422 in the second column of Supplementary Table 2), the model with a distinct shape for
423 Domestic and Wild populations is accepted only in two, rather unrelated, scenarios (scenarios
424 7 and 14). This indicates that an artificial alteration in the shape of the deleterious DFE
425 between Domestic and Wild populations can be inferred. Fortunately, when comparing
426 models that take into account beneficial mutations (models M2 vs M20, third column in
427 Supplementary Table 2), all scenarios show a shared shape of the deleterious DFE, which is
428 expected based on the simulation parameters. These findings suggest that disregarding
429 beneficial mutations can cause an artificial change in the inferred shape of the marginal
430 deleterious DFE between populations, as noted previously by Tataru et al. in 2017. Second,

431 incorporating the positive DFE yields statistically significant results in all scenarios (see
432 Supplementary Table 2, fourth and fifth columns). Hence, polyDFE appears to effectively
433 detect beneficial mutations, regardless of the strength of positive selection. Third, we
434 investigate whether Domestic and Wild populations could exhibit an artificial change in the
435 beneficial DFEs as a consequence of domestication. When comparing the M20 and M30
436 models (refer to the last column in Supplementary Table 2), polyDFE invokes changes in the
437 positive DFE between populations in some scenarios. This is applicable when there is no
438 migration between the populations and only a minimal amount (5%) or when none of the
439 sites change their selection coefficient, regardless of the mean strength of positive selection.
440 These artificial changes occur in scenarios 2, 7, 8, 13, and 14, with a marginal p-value in
441 scenario 1. It is noteworthy that the polyDFE analysis shows no significant difference in the
442 positive DFE between populations with the presence of migration and when p_C equals 25%.
443 Our initial expectation was that in scenarios with a large fraction of sites changing selection
444 coefficients and migration from the Wild population, would result in an increase in the load
445 of advantageous polymorphisms in the Domestic population (due to the re-introduction of
446 beneficial mutations from the Wild to the Domestic population), leading to a higher inferred
447 rate of new advantageous mutations (p_b) compared to the Wild population. We do not
448 observe this result. We suspect that the absence of this result could be due to linkage between
449 selected mutations and synonymous mutations, which may lead to an overcorrection of the
450 excess of non-synonymous polymorphisms at high frequency via the r_i parameters.

451 polyDFE suggests that specific domestication scenarios, particularly those lacking migration
452 and featuring minimal changes in selection coefficients, may artificially alter the marginal full
453 DFE between populations, particularly in its positive side. In the next section, we find that the
454 artificial change in the marginal full DFE is due to the detection of a higher proportion of new,
455 effectively neutral, advantageous mutations (>10%) in Domestic populations compared to
456 Wild populations. Hence, this finding has no significant impact on the marginal full DFE
457 differences between the populations when the DFE is represented in discrete intervals. We
458 demonstrate that domestication does not significantly impact polyDFE's ability to detect a false
459 difference in the marginal full DFE among populations. We conclude that if a significant
460 change is detected in the discretized marginal full DFE, it must be considered valid.

461 **Estimation of DFE parameters in Wild and Domestic populations**

462 Under the polyDFE framework, we begin by extracting the Akaike Information Criterion (AIC)
463 from every model (Table 3) and then computing the AIC-weighted parameters for all models
464 (Tataru and Bataillon 2019; Castellano *et al.* 2019). This approach is used because the true
465 model generating real data in both Wild and Domestic populations is unknown. Instead, under
466 *dadi*'s framework, we adopt an alternative methodology that utilizes very general, parameter
467 rich and versatile joint demographic and DFE models to fit the 2D-SFS. The diagnostic plots
468 of the new joint DFE model is shown in Supplementary Figure 1, again there is good agreement
469 between the model fits and the data.

470

471 Figure 3 depicts the distribution of parameters related to the deleterious DFE that are estimated
472 by performing bootstrap analysis using polyDFE and *dadi*. We observe that both tools have a
473 tendency to marginally overestimate the shape parameter of the gamma distribution employed
474 to model the deleterious DFE. The overestimation is particularly significant in polyDFE, when
475 positive selection is rare and strong. In such scenarios, *dadi*'s shape estimation is sometimes
476 rather noisy. Regarding the mean of the deleterious (s_d), we observe quite accurate inferences
477 with both tools across domestication scenarios. This finding indicates that regardless of the
478 inference method used, the estimation of the deleterious DFE is resilient to demographic and
479 selective changes, as well as the pervasive impact of linked selection. In contrast, our previous
480 inference with *dadi* on the demographic parameters concluded that linked selection
481 significantly complicates the process of obtaining accurate demographic histories. Therefore,
482 although it is generally believed that demographic changes should be considered to infer the
483 underlying DFE, we found that inferring the deleterious DFE is "easier" than inferring the true
484 demographic history. We conclude that correcting the non-synonymous SFS through nuisance
485 r_i parameters or using a demographic history that fits the data well, even if it is incorrect,
486 appears sufficient for obtaining an accurate depiction of the deleterious DFE.

487 The distribution of parameters associated with the beneficial DFE, estimated by bootstrap
488 analysis using polyDFE and *dadi*, is shown in Supplementary Figure 4 and Supplementary
489 Table 3. Depending on the scenario, we simulate an average increase in relative fitness (s_b) of
490 1%, 0.1%, and 0.01%. Positive selection's strength is usually substantially underestimated by
491 polyDFE and *dadi*, but only polyDFE consistently overestimates the proportion of new
492 advantageous mutations (p_b), regardless of the true simulated value. Supplementary Figure 5

493 displays the discretized full DFE. Given the distribution of inferred values of p_b and s_b, we
494 reason that a peak of effectively neutral advantageous mutations is being measured by
495 polyDFE. The overall excess of effectively neutral advantageous mutations measured by
496 polyDFE is generally balanced by the defect of effectively neutral deleterious mutations.
497 Consequently, polyDFE seems to have limited power in identifying effectively beneficial
498 mutations on the 1D-SFS (under these simulation conditions). As suggested before, the r_i
499 parameters might be overcorrecting for the increase in high-frequency non-synonymous
500 polymorphisms in the SFS expected from beneficial mutations. By the same logic, *dadi's*
501 inferred demographic history might be operating in a similar way to explain the uptick of
502 synonymous polymorphisms at high frequency due to linkage to beneficial mutations. Thus,
503 we conclude that both tools struggle to infer the positive DFE and tend to be overconservative
504 and identify weaker positive selection than what has been simulated. However, it is noteworthy
505 that both tools typically yield comparable (and reasonably accurate) discretized deleterious
506 DFEs upon considering the tendency of polyDFE to infer a peak of effectively neutral
507 beneficial mutations.

508 **Estimation of the fraction of mutations with divergent selective effects (p_c) between**
509 **Domestic and Wild populations**

510 One of the main goals of this study is to determine the proportion of new and
511 standing non-synonymous mutations with differing selection coefficients in Wild and
512 Domestic populations. The usage of our new joint DFE model is not limited to the current
513 study. Our new model, created by mixing multiple distributions to mimic mutation types in our
514 simulations (Table 2; Figure 1C-D), is suitable for usage in any recently diverged populations.
515 Hence, while we acknowledge that our simulation and inference pipeline has the potential to
516 provide insights into recent parapatric and allopatric speciation events, our primary focus in
517 this work is on assessing our ability to identify the impact of domestication on the full DFE
518 within domesticated populations. This emphasis is due to the availability of independent
519 archaeological evidence that can be used to determine the timing of domestication onset.

520 Figure 4 displays the distribution of the inferred p_c for three different positive DFEs, along
521 with simulated p_c values. When positive selection is not strong, it becomes apparent that
522 scenarios with a significant fraction of mutations with dissimilar selective effects (p_c = 25%)
523 can readily be differentiated from those where a small (p_c = 5%) or nonexistent (p_c = 0%)

number of sites alter their selection coefficient. However, differentiating our negative control from a positive control proves difficult when only 5% of the sites show a difference in their selection coefficients. Notably, we overestimate p_C significantly in cases of strong positive selection, indicating that hard selective sweeps may mimic divergent selection in a substantial amount of non-synonymous mutations. We observe no major impact of migration on the inferred p_C values across scenarios.

The overestimation of p_C when positive selection is strong is not surprising, since mutations with stable selection coefficients between populations may be in close recombinational proximity and can hitchhike with strongly beneficial mutations that are population-specific. This will exacerbate the apparent fraction of mutations with divergent selective effects. In contrast, if positive selection is weaker, recombination will be able to disentangle beneficial mutations from the rest of mutation types and simplify our estimation of p_C. One way to ameliorate this problem would be to remove genomic windows with evidence of recent population-specific, complete or partial, selective sweeps and rerun our inference pipeline. For example, these could be regions with low neutral genetic diversity. However, we find this heuristic solution might be difficult to implement in practice.

Supplementary Figure 6 shows the observed level of neutral genetic diversity (measured using Watterson's theta and synonymous sites, θ_S) and the selective constraint (i.e., the ratio of non-synonymous polymorphisms to synonymous polymorphisms per site, P_n/P_s) for each independent simulation run. Note the large decrease in the observed θ_S, driven entirely by linked selection in Wild populations, relative to the expected level of neutral genetic diversity (expected θ_S = 0.005 under free recombination). Particularly important is the reduction in the average θ_S across independent simulation runs in Wild populations when positive selection is rare and strong (θ_S is ~20% of the expected value), whereas when positive selection is weaker (and perhaps absent if S_b = 1) the observed level of genetic diversity is ~~reduced to~~ ~40% of the expected value. In strong positive selection scenarios, there may be no heuristic correction or genomic region that escapes *genetic draft* (Gillespie 2000), and our current definition and interpretation of p_C would be misleading. We also observe that although synonymous genetic diversity and the selective constraint is higher in Wild populations than in Domestic populations, Wild populations show more variability in θ_S and P_n/P_s across independent simulation runs. This is likely explained by both the higher chance of sampling strongly

555 beneficial mutations and the greater selection efficacy expected in the constant population size
556 of Wild populations. Moreover, relative to Domestic populations, we find that a higher p_C
557 always corresponds to a lower θ_S and selective constraint (all else being equal). The largest
558 difference in the level of genetic diversity and P_n/P_s between Domestic and Wild populations
559 occurs when the simulated p_C is substantial (25%), and S_b is less than 100. Thus, for a given
560 joint demographic history, there appears to be a positive relationship between the simulated p_C
561 and the difference in genetic diversity and selective constraint between Wild and Domestic
562 populations. This observation only applies when positive selection is not strong. When positive
563 selection is strong, genetic diversity and selective pressure are significantly further reduced in
564 both Domestic and Wild populations, causing the two distributions to largely overlap. As
565 described above for the reconstruction of demographic history, when selective sweeps are
566 strong, the recovered demographic history also tends to overlap between Wild and Domestic
567 populations. The overlap of demographic histories and neutral genetic diversity distributions
568 could be used as a caution signal and as an indicator of strong positive selection and widespread
569 genetic draft. Finally, migration appears to cause a minor reduction in P_n/P_s and increase
570 genetic diversity within Domestic populations. Thus, migration acts slightly diminishing the
571 P_n/P_s discrepancy between Wild and Domestic populations.

572 **Implications for empirical analysis of populations**

573 Although the time of separation between wild and domestic is recent, the external environments
574 in which they live are very different. This means that an unspecified proportion of
575 environmentally influenced variants may have changed their fitness effect in the domestic
576 population, which may have altered their frequencies. In this work, we simulated differential
577 effects between wild and domestic populations, and we observed that selective effects affect
578 the inference of demographic parameters by linked selection, but to different extents depending
579 on the DFE. Linked selection caused by positive effects is responsible for strong differences
580 from the true parameters, even if they are very rare but strong. Nevertheless, the DFE can be
581 estimated quite accurately, suggesting that methods that infer the entire DFE can be used first
582 and then estimate the demographic parameters using this information.

583 Another point of interest for empirical geneticists is the development of a new method to jointly
584 infer the DFE between wild and domestic and their differences in the positive part of the
585 distribution. The 2D dadi extension algorithm allows to infer differences in p+w (the fraction

586 of mutations that are positively selected in the wild population), pc (the fraction of mutations
587 that change the coefficient of selection in the domestic population), pc+ (the fraction of those
588 mutations that become beneficial in the domestic population).

589

CONCLUSIONS

In summary, our use of forward-in-time simulations has provided valuable insights into the complex genetic demographic history and distribution of fitness effects (DFE) for both new and standing amino acid mutations in the context of domestication. Through a comparative analysis of two methods, polyDFE and *dadi*, we have uncovered the impact of linked selection on the reconstructed demographic history of both wild and domesticated populations. Despite biases in the timelines of domestication events and bottleneck characteristics, the estimation of deleterious DFE remains remarkably reliable, demonstrating the robustness of these analytical approaches. In particular, the underestimation of effectively beneficial mutations in the DFE highlights the influence of linkage between beneficial and neutral mutations, which requires careful consideration in model interpretation. In addition, our results shed light on distinguishing scenarios of divergent selective effects between populations under weak and strong positive selection, providing a nuanced understanding of the interplay of evolutionary forces. As we navigate the complex landscape of domestication, these methodological approaches contribute significantly to unraveling the evolutionary dynamics and adaptive processes that shape the genomes of domesticated organisms, and provide a foundation for future research in this critical area of study.

Supplementary Information

We have added the Diagnostic plots 2D-SFS for synonymous and Nonsynonymous positions obtained with *dadi* for all the scenarios analyzed, plus six additional Figures and three additional Tables in the Supplementary Material. The scripts used in the analyses of this work were uploaded in Github, available at the link https://github.com/CastellanoED/domesticationDFE.

Acknowledgments

SERO. was supported by grants AGL2016-78709-R (MEC, Spain) and PID2020-119255GB-I00 (MICINN, Spain), by the CERCA Programme/Generalitat de Catalunya and acknowledges financial support from the Spanish Ministry of Economy and Competitiveness, through the Severo Ochoa Programme for Centres of Excellence in R&D 2016-2019 and 2020-2023 (SEV-2015-0533, CEX2019-000917) and the European Regional Development Fund (ERDF). RNG and DC were supported by the National Institute of General Medical Sciences of the National Institutes of Health (R35GM149235 and R01GM127348 to RNG). ITV was supported by a predoctoral fellowship funded by MCIN/AEI/ 10.13039/501100011033 through the Grant BES-2017-081139 and by "ESF Investing in your future". This research was also supported by NSF Grant No. PHY-1748958 and the Gordon and Betty Moore Foundation Grant No. 2919.02.

LITERATURE CITED

Anaconda Software Distribution. Computer software. Vers. 2-2.4.0. Anaconda, Nov. 2016. Web.

Ahmad H. I., M. J. Ahmad, F. Jabbir, S. Ahmar, N. Ahmad, *et al.*, 2020 The Domestication Makeup: Evolution, Survival, and Challenges. Front. Ecol. Evol. 8.

Amills M., H. J. W. C. Megens, A. Manunza, S. E. Ramos-Onsins, and M. Groenen, 2017 A genomic perspective about wild boar demography and evolution, pp. 376–387 in *Ecology, Conservation and Management of Wild Pigs and Peccaries*, Cambridge University Press.

Andersson L., 2012 Genetics of Animal Domestication, pp. 260–274 in *Biodiversity in Agriculture: Domestication, Evolution, and Sustainability*, edited by Damania A. B., Qualset C. O., McGuire P. E., Gepts P., Bettinger R. L., *et al.* Cambridge University Press, Cambridge.

Arnoux S, Fraïsse C, Sauvage C. Genomic inference of complex domestication histories in three Solanaceae species. J Evol Biol. 2021 Feb;34(2):270-283. doi: 10.1111/jeb.13723. Epub 2020 Nov 10. PMID: 33107098.

Avni R., M. Nave, O. Barad, K. Baruch, S. O. Twardziok, *et al.*, 2017 Wild emmer genome architecture and diversity elucidate wheat evolution and domestication. Science 357: 93–97. https://doi.org/10.1126/science.aan0032

Barghi N., R. Tobler, V. Nolte, A. M. Jakšić, F. Mallard, *et al.*, 2019 Genetic redundancy fuels polygenic adaptation in Drosophila. PLOS Biol. 17: e3000128. https://doi.org/10.1371/journal.pbio.3000128

Barton H. J., and K. Zeng, 2018 New Methods for Inferring the Distribution of Fitness Effects for INDELs and SNPs. Mol. Biol. Evol. 35: 1536–1546. https://doi.org/10.1093/molbev/msy054

Beissinger TM, Wang L, Crosby K, Durvasula A, Hufford MB, Ross-Ibarra J. Recent demography drives changes in linked selection across the maize genome. Nat Plants. 2016 Jun 13;2:16084. doi: 10.1038/nplants.2016.84. PMID: 27294617.

657 Berg J. J., and G. Coop, 2014 A population genetic signal of polygenic adaptation. PLoS Genet.
658 10: e1004412. https://doi.org/10.1371/journal.pgen.1004412

659 Birky CW Jr, Walsh JB. Effects of linkage on rates of molecular evolution. Proc Natl Acad Sci
660 U S A. 1988 Sep;85(17):6414-8. doi: 10.1073/pnas.85.17.6414.

661 Boyko A. R., R. H. Boyko, C. M. Boyko, H. G. Parker, M. Castelhano, et al., 2009 Complex
662 population structure in African village dogs and its implications for inferring dog domestication
663 history. Proc. Natl. Acad. Sci. U. S. A. 106: 13903–13908.
664 https://doi.org/10.1073/pnas.0902129106

665 Caicedo AL, Williamson SH, Hernandez RD, Boyko A, Fledel-Alon A, York TL, Polato NR,
666 Olsen KM, Nielsen R, McCouch SR, Bustamante CD, Purugganan MD. Genome-wide patterns
667 of nucleotide polymorphism in domesticated rice. PLoS Genet. 2007 Sep;3(9):1745-56. doi:
668 10.1371/journal.pgen.0030163. Epub 2007 Aug 6.

669 Castellano D., M. C. Macià, P. Tataru, T. Bataillon, and K. Munch, 2019 Comparison of the
670 Full Distribution of Fitness Effects of New Amino Acid Mutations Across Great Apes.
671 Genetics 213: 953–966. https://doi.org/10.1534/genetics.119.302494

672 Chen Q, Samayoa LF, Yang CJ, Olukolu BA, York AM, Sanchez-Gonzalez JJ, Xue W,
673 Glaubitz JC, Bradbury PJ, Romay MC, Sun Q, Buckler ES, Holland JB, Doebley JF. A
674 conserved genetic architecture among populations of the maize progenitor, teosinte, was
675 radically altered by domestication. Proc Natl Acad Sci U S A. 2021 Oct
676 26;118(43):e2112970118. doi: 10.1073/pnas.2112970118. PMID: 34686607; PMCID:
677 PMC8639367.

678 Coffman A. J., P. H. Hsieh, S. Gravel, and R. N. Gutenkunst, 2016 Computationally Efficient
679 Composite Likelihood Statistics for Demographic Inference. Mol. Biol. Evol. 33: 591–593.
680 https://doi.org/10.1093/molbev/msv255

681 Comeron JM. Background selection as null hypothesis in population genomics: insights and
682 challenges from Drosophila studies. Philos Trans R Soc Lond B Biol Sci. 2017 Dec
683 19;372(1736):20160471. doi: 10.1098/rstb.2016.0471. PMID: 29109230; PMCID:
684 PMC5698629.

Courtier-Orgogozo V., and A. Martin, 2020 The coding loci of evolution and domestication: current knowledge and implications for bio-inspired genome editing, (M. H. Dickinson, 27 L. B. Vosshall, and J. A. T. Dow, Eds.). J. Exp. Biol. 223: jeb208934. https://doi.org/10.1242/jeb.208934

Crow J. F., and M. Kimura, 1979 Efficiency of truncation selection*. Proc. Natl. Acad. Sci. U. S. A. 76: 396–399. Dayan T., 1994 Early Domesticated Dogs of the Near East. J. Archaeol. Sci. 21: 633–640. https://doi.org/10.1006/jasc.1994.1062

Devi A., and K. Jain, 2023 Polygenic adaptation dynamics in large, finite populations. 2023.01.25.525607. Driscoll C. A., D. W. Macdonald, and S. J. O'Brien, 2009 From wild animals to domestic pets, an evolutionary view of domestication. Proc. Natl. Acad. Sci. 106: 9971–9978. https://doi.org/10.1073/pnas.0901586106

Frantz L. A. F., J. G. Schraiber, O. Madsen, H.-J. Megens, A. Cagan, *et al.*, 2015 Evidence of long-term gene flow and selection during domestication from analyses of Eurasian wild and domestic pig genomes. Nat. Genet. 47: 1141–1148. https://doi.org/10.1038/ng.3394

Galtier N. Adaptive Protein Evolution in Animals and the Effective Population Size Hypothesis. PLoS Genet. 2016 Jan 11;12(1):e1005774. doi: 10.1371/journal.pgen.1005774. PMID: 26752180; PMCID: PMC4709115.

Gillespie J. H., 2000 Genetic drift in an infinite population. The pseudohitchhiking model. Genetics 155: 909–919. https://doi.org/10.1093/genetics/155.2.909

Granleese T., S. A. Clark, and J. H. J. van der Werf, 2019 Genotyping strategies of selection candidates in livestock breeding programmes. J. Anim. Breed. Genet. 136: 91–101. https://doi.org/10.1111/jbg.12381

Groenen M. A. M., A. L. Archibald, H. Uenishi, C. K. Tuggle, Y. Takeuchi, *et al.*, 2012 Analyses of pig genomes provide insight into porcine demography and evolution. Nature 491: 393–398. https://doi.org/10.1038/nature11622

Gutenkunst R. N., R. D. Hernandez, S. H. Williamson, and C. D. Bustamante, 2009 Inferring the Joint Demographic History of Multiple Populations from Multidimensional SNP Frequency Data. PLOS Genet. 5: e1000695. https://doi.org/10.1371/journal.pgen.1000695

Haller B. C., and P. W. Messer, 2023 SLiM 4: Multispecies Eco-Evolutionary Modeling. Am. Nat. 201: E127–E139. https://doi.org/10.1086/723601

He Y., Y. Guo, W. Zheng, T. Yue, H. Zhang, *et al.*, 2023 Polygenic adaptation leads to a higher reproductive fitness of native Tibetans at high altitude. Curr. Biol. CB 33: 4037-4051.e5. https://doi.org/10.1016/j.cub.2023.08.021

Huang X., N. Kurata, X. Wei, Z.-X. Wang, A. Wang, *et al.*, 2012 A map of rice genome variation reveals the origin of cultivated rice. Nature 490: 497–501. https://doi.org/10.1038/nature11532

Huang X., A. L. Fortier, A. J. Coffman, T. J. Struck, M. N. Irby, *et al.*, 2021 Inferring Genome-Wide Correlations of Mutation Fitness Effects between Populations. Mol. Biol. Evol. 38: 4588–4602. https://doi.org/10.1093/molbev/msab162

Jain K., and W. Stephan, 2017a Rapid Adaptation of a Polygenic Trait After a Sudden Environmental Shift. Genetics 206: 389–406. https://doi.org/10.1534/genetics.116.196972

Jain K., and W. Stephan, 2017b Modes of Rapid Polygenic Adaptation. Mol. Biol. Evol. 34: 3169–3175. https://doi.org/10.1093/molbev/msx240

Jerison E. R., S. Kryazhimskiy, and M. M. Desai, 2014 Pleiotropic consequences of adaptation across gradations of environmental stress in budding yeast

Keightley P. D., and A. Eyre-Walker, 2007 Joint inference of the distribution of fitness effects of deleterious mutations and population demography based on nucleotide polymorphism frequencies. Genetics 177: 2251–2261. https://doi.org/10.1534/genetics.107.080663

Kim B. Y., C. D. Huber, and K. E. Lohmueller, 2017 Inference of the Distribution of Selection Coefficients for New Nonsynonymous Mutations Using Large Samples. Genetics 206: 345–361. https://doi.org/10.1534/genetics.116.197145

Kondrashov A. S., 1988 Deleterious mutations and the evolution of sexual reproduction. Nature 336: 435–440. https://doi.org/10.1038/336435a0

Larson G., and J. Burger, 2013 A population genetics view of animal domestication. Trends Genet. TIG 29: 197–205. https://doi.org/10.1016/j.tig.2013.01.003

Larson G., D. R. Piperno, R. G. Allaby, M. D. Purugganan, L. Andersson, *et al.*, 2014 Current perspectives and the future of domestication studies. Proc. Natl. Acad. Sci. 111: 6139–6146. https://doi.org/10.1073/pnas.1323964111

Leno-Colorado J., S. Guirao-Rico, M. Pérez-Enciso, and S. E. Ramos-Onsins, 2022 Pervasive selection pressure in wild and domestic pigs. 2020.09.09.289439.

Li N., R. Xu, P. Duan, and Y. Li, 2018 Control of grain size in rice. Plant Reprod. 31: 237–251. https://doi.org/10.1007/s00497-018-0333-6

Librado P., N. Khan, A. Fages, M. A. Kusliy, T. Suchan, *et al.*, 2021 The origins and spread of domestic horses from the Western Eurasian steppes. Nature 598: 634–640. https://doi.org/10.1038/s41586-021-04018-9

Lozano R, Gazave E, Dos Santos JPR, Stetter MG, Valluru R, Bandillo N, Fernandes SB, Brown PJ, Shakoor N, Mockler TC, Cooper EA, Taylor Perkins M, Buckler ES, Ross-Ibarra J, Gore MA. Comparative evolutionary genetics of deleterious load in sorghum and maize. Nat Plants. 2021 Jan;7(1):17-24. doi: 10.1038/s41477-020-00834-5. Epub 2021 Jan 15. PMID: 33452486.

Lu J., T. Tang, H. Tang, J. Huang, S. Shi, *et al.*, 2006 The accumulation of deleterious mutations in rice genomes: a hypothesis on the cost of domestication. Trends Genet. 22: 126–131. https://doi.org/10.1016/j.tig.2006.01.004

Marsden C. D., D. Ortega-Del Vecchyo, D. P. O'Brien, J. F. Taylor, O. Ramirez, *et al.*, 2016 Bottlenecks and selective sweeps during domestication have increased deleterious genetic variation in dogs. Proc. Natl. Acad. Sci. 113: 152–157. https://doi.org/10.1073/pnas.1512501113

Morell Miranda P, Soares AER, Günther T. Demographic reconstruction of the Western sheep expansion from whole-genome sequences. G3 (Bethesda). 2023 Nov 1;13(11):jkad199. doi: 10.1093/g3journal/jkad199. PMID: 37675574.

Moyers, Morrell, and McKay, 2018 Genetic Costs of Domestication and Improvement. J. Hered. 109. https://doi.org/10.1093/jhered/esx069 Murray C., E. Huerta-Sanchez, F. Casey, and D. G. Bradley, 2010 Cattle demographic history modelled from autosomal sequence

variation. Philos. Trans. R. Soc. B Biol. Sci. 365: 2531–2539. https://doi.org/10.1098/rstb.2010.0103

Murray C, Huerta-Sanchez E, Casey F, Bradley DG. Cattle demographic history modelled from autosomal sequence variation. Philos Trans R Soc Lond B Biol Sci. 2010 Aug 27;365(1552):2531-9. doi: 10.1098/rstb.2010.0103. PMID: 20643743; PMCID: PMC2935105.

Nielsen R., 2005 Molecular signatures of natural selection. Annu. Rev. Genet. 39: 197–218. https://doi.org/10.1146/annurev.genet.39.073003.112420

Ohta T., 1989 The mutational load of a multigene family with uniform members. Genet. Res. 53: 141–145. https://doi.org/10.1017/s0016672300028020

Pacifici M., L. Santini, M. D. Marco, D. Baisero, L. Francucci, *et al.*, 2013 Generation length for mammals. Nat. Conserv. 5: 89–94. https://doi.org/10.3897/natureconservation.5.5734 polyDFE/tutorial.pdf at master · paula-tataru/polyDFE, GitHub. Pritchard J. K., J. K. Pickrell, and G. Coop, 2010 The Genetics of Human Adaptation: Hard Sweeps, Soft Sweeps, and Polygenic Adaptation. Curr. Biol. 20: R208–R215. https://doi.org/10.1016/j.cub.2009.11.055

Purugganan M. D., and D. Q. Fuller, 2009 The nature of selection during plant domestication. Nature 457: 843–848. https://doi.org/10.1038/nature07895

Ragsdale A. P., A. J. Coffman, P. Hsieh, T. J. Struck, and R. N. Gutenkunst, 2016 Triallelic Population Genomics for Inferring Correlated Fitness Effects of Same Site Nonsynonymous Mutations. Genetics 203: 513–523. https://doi.org/10.1534/genetics.115.184812

Raybaut, P. (2009). Spyder-documentation. *Available Online at: Pythonhosted. Org*. Redding R. W., 2015 The Pig and the Chicken in the Middle East: Modeling Human Subsistence Behavior in the Archaeological Record Using Historical and Animal Husbandry Data. J. Archaeol. Res. 23: 325–368. https://doi.org/10.1007/s10814-015-9083-2

Reid B. N., B. Star, and M. L. Pinsky, 2023 Detecting parallel polygenic adaptation to novel evolutionary pressure in wild populations: a case study in Atlantic cod (Gadus morhua). Philos. Trans. R. Soc. B Biol. Sci. 378: 20220190. https://doi.org/10.1098/rstb.2022.0190

Rossum G. V., and F. L. Drake, 2009 *Python 3 Reference Manual: (Python Documentation Manual Part 2)*. CreateSpace Independent Publishing Platform.

Rubin C.-J., M. C. Zody, J. Eriksson, J. R. S. Meadows, E. Sherwood, *et al.*, 2010 Whole-genome resequencing reveals loci under selection during chicken domestication. Nature 464: 587–591. https://doi.org/10.1038/nature08832

Shomura A., T. Izawa, K. Ebana, T. Ebitani, H. Kanegae, *et al.*, 2008 Deletion in a gene associated with grain size increased yields during rice domestication. Nat. Genet. 40: 1023–1028. https://doi.org/10.1038/ng.169

Stephan W., 2016 Signatures of positive selection: from selective sweeps at individual loci to subtle allele frequency changes in polygenic adaptation. Mol. Ecol. 25: 79–88. https://doi.org/10.1111/mec.13288

Stephan W., and S. John, 2020 Polygenic Adaptation in a Population of Finite Size. Entropy 22: 907. https://doi.org/10.3390/e22080907

Tataru P., M. Mollion, S. Glémin, and T. Bataillon, 2017 Inference of Distribution of Fitness Effects and Proportion of Adaptive Substitutions from Polymorphism Data. Genetics 207: 1103–1119. https://doi.org/10.1534/genetics.117.300323

Tataru P., and T. Bataillon, 2019 polyDFEv2.0: testing for invariance of the distribution of fitness effects within and across species. Bioinforma. Oxf. Engl. 35: 2868–2869. https://doi.org/10.1093/bioinformatics/bty1060

Todd E. T., L. Tonasso-Calvière, L. Chauvey, S. Schiavinato, A. Fages, *et al.*, 2022 The genomic history and global expansion of domestic donkeys. Science 377: 1172–1180. https://doi.org/10.1126/science.abo3503

Torres R, Stetter MG, Hernandez RD, Ross-Ibarra J. The Temporal Dynamics of Background Selection in Nonequilibrium Populations. Genetics. 2020 Apr;214(4):1019-1030. doi: 10.1534/genetics.119.302892. Epub 2020 Feb 18. PMID: 32071195; PMCID: PMC7153942.

Van Laere A.-S., M. Nguyen, M. Braunschweig, C. Nezer, C. Collette, *et al.*, 2003 A regulatory mutation in IGF2 causes a major QTL effect on muscle growth in the pig. Nature 425: 832–836. https://doi.org/10.1038/nature02064

Vladar H. P. de, and N. Barton, 2014 Stability and response of polygenic traits to stabilizing selection and mutation. Genetics 197: 749–767. https://doi.org/10.1534/genetics.113.159111

Wright S. I., I. V. Bi, S. G. Schroeder, M. Yamasaki, J. F. Doebley, *et al.*, 2005 The effects of artificial selection on the maize genome. Science 308: 1310–1314. https://doi.org/10.1126/science.1107891

Yang J., W.-R. Li, F.-H. Lv, S.-G. He, S.-L. Tian, *et al.*, 2016 Whole-Genome Sequencing of Native Sheep Provides Insights into Rapid Adaptations to Extreme Environments. Mol. Biol. Evol. 33: 2576–2592. https://doi.org/10.1093/molbev/msw129

Zeder M. A., E. Emshwiller, B. D. Smith, and D. G. Bradley, 2006 Documenting domestication: the intersection of genetics and archaeology. Trends Genet. TIG 22: 139–155. https://doi.org/10.1016/j.tig.2006.01.007

Zeder M. A., 2012 The Domestication of Animals. J. Anthropol. Res. 68: 161–190. https://doi.org/10.3998/jar.0521004.0068.201

Zeder M. A., 2015 Core questions in domestication research. Proc. Natl. Acad. Sci. 112: 3191–3198. https://doi.org/10.1073/pnas.1501711112

839 **Table 1**

840 **Variable demographic and selective parameters across scenarios**

Positive DFE*	Migration (W>D)	p_c	Scenario ID
p_b =10%& S_b = 1	0%	0%	1
		5%	2
		25%	3
Pervasive and nearly neutral	1%	0%	4
		5%	5
		25%	6
p_b = 1% & S_b = 10	0%	0%	7
		5%	8
		25%	9
Common and weak	1%	0%	10
		5%	11
		25%	12
p_b = 0.1% & S_b = 100	0%	0%	13
		5%	14
		25%	15
Rare and strong	1%	0%	16
		5%	17
		25%	18

841 * The eighteen simulated combinations of parameters in this study. The first column refers to the DFE of new
842 beneficial mutations, the second column represents the migration rate from the Wild to the Domestic population
843 and the third column shows the percentage of sites that change their selection coefficients in the Domestic
844 population (p_c). Last column shows the ID we use to quickly label scenarios along the manuscript.

845

846 **Table 2**

847 **Types of sites in simulated scenarios**

Site	Wild	Domestic
m1	Neutral	No change, remain Neutral
m2	Beneficial	No change, remain Beneficial
m3	Beneficial	Change to a different Beneficial Effect
m4	Beneficial	Change to Deleterious
m5	Deleterious	No change, remain Deleterious
m6	Deleterious	Change to a different Deleterious Effect
m7	Deleterious	Change to Beneficial

848

849 **Table 3**

850 **List of nested polyDFE models and (co)estimated parameters.**

Model ID*	Negative DFE		Positive DFE	
	shape	S_d	p_b	S_b
M1	Var†	Var	-	-
M10	Fix¶	Var	-	-
M2	Var	Var	Var	Var
M20	Fix	Var	Var	Var
M30	Fix	Var	Fix	Fix

851 *The population mutation rate (Θ), the nuisance parameters (r_i) and the mispolarization parameter (ε) are all
852 independently estimated across Wild and Domestic populations. S_d is always independently estimated to
853 accommodate potential changes in N_e between populations. †(Var) Independently estimated parameters for the
854 Domestic and Wild populations. ¶(Fix) Jointly estimated parameters for the Domestic and Wild populations.

855
856

857 **FIGURE LEGENDS**

858 **Figure 1.** Joint demographic and DFE models simulated and fit. A: Illustration of the joint
859 demographic model used in SLiM simulations. Na: Effective population size of the Ancestral
860 population. New: Effective population size of the Wild population. Ne1d: Effective population
861 size of the Domestic population during the bottleneck. Ne2d: Effective population size of the
862 Domestic population after the bottleneck. T1: Number of generations in the bottleneck period.
863 T2: Number of generations from the bottleneck to the present. m: Wild to Domestic migration
864 rate (migration occurs along T1). B: Illustration of a more general joint demographic model
865 used in the dadi inferences. Na: Effective population size of the Ancestral population. Npre:
866 Effective population size before the domestication split. N1div: Effective population size of
867 the Wild population after the split. N1F: Effective population size of the Wild population at the
868 end of the simulation. N2div: Effective population size of the Domestic population after the
869 split. N2F: Effective population size of the Domestic population at the end of the simulation.
870 Tpre: Number of generations before the domestication split. Tdiv: Number of generations after
871 the bottleneck. T1F: Number of generations under N1F. T2F: Number of generations under
872 N2F. Note that T1F and T2F are estimated independently and that T1F can be the same, longer
873 or shorter than T2F. md: Wild to Domestic migration rate. mw: Domestic to Wild migration
874 rate. Both migration rates occur after the domestication split. C: Illustration of the joint DFE
875 model used in the SLiM simulations, with mutation types illustrated. D: Illustration of the joint
876 DFE model used in the dadi inferences, in which a fixed positive selection coefficient is
877 assumed.

878 **Figure 2.** Solid lines showing the inferred demographic histories for the eighteen simulated
879 scenarios. In salmon the Wild population and in light-blue the Domestic population. The dashed
880 line shows the true simulated demography in Domestic populations. The true Wild population
881 is not shown but it is a constant population size with relative Ne = 1. The 95% confidence
882 intervals calculated using the Godambe approximation can be found in Supplementary Table
883 1.

884 **Figure 3.** Sampling distributions of estimated parameters for the deleterious DFE are obtained
885 using 100 bootstrap replicates. Dotted vertical lines indicate the actual simulated parameter
886 values. A) Shape parameter estimated with polyDFE in dark gray the Wild population and in
887 light gray the Domestic population, B) shape parameter estimated with dadi, C) mean sd
888 estimated with polyDFE in dark gray the Wild population and in light gray the Domestic

population and D) mean sd estimated with dadi. To calculate sd from inferred Sd values, we divided Sd by 4 times the Ne estimate in polyDFE and by 2 times the Na estimate in dadi. To obtain the Ne (and Na) we divide π at synonymous sites by the true simulated mutation rate (2.5x10-7 per site and generation). Note that dadi uses the joint demographic model parameters to compute π at synonymous sites, while polyDFE assumes a constant population size.

Figure 4. Sampling distributions of inferred pc are obtained using 100 bootstrap replicates. In light green scenarios without migration and in dark green scenarios with migration.

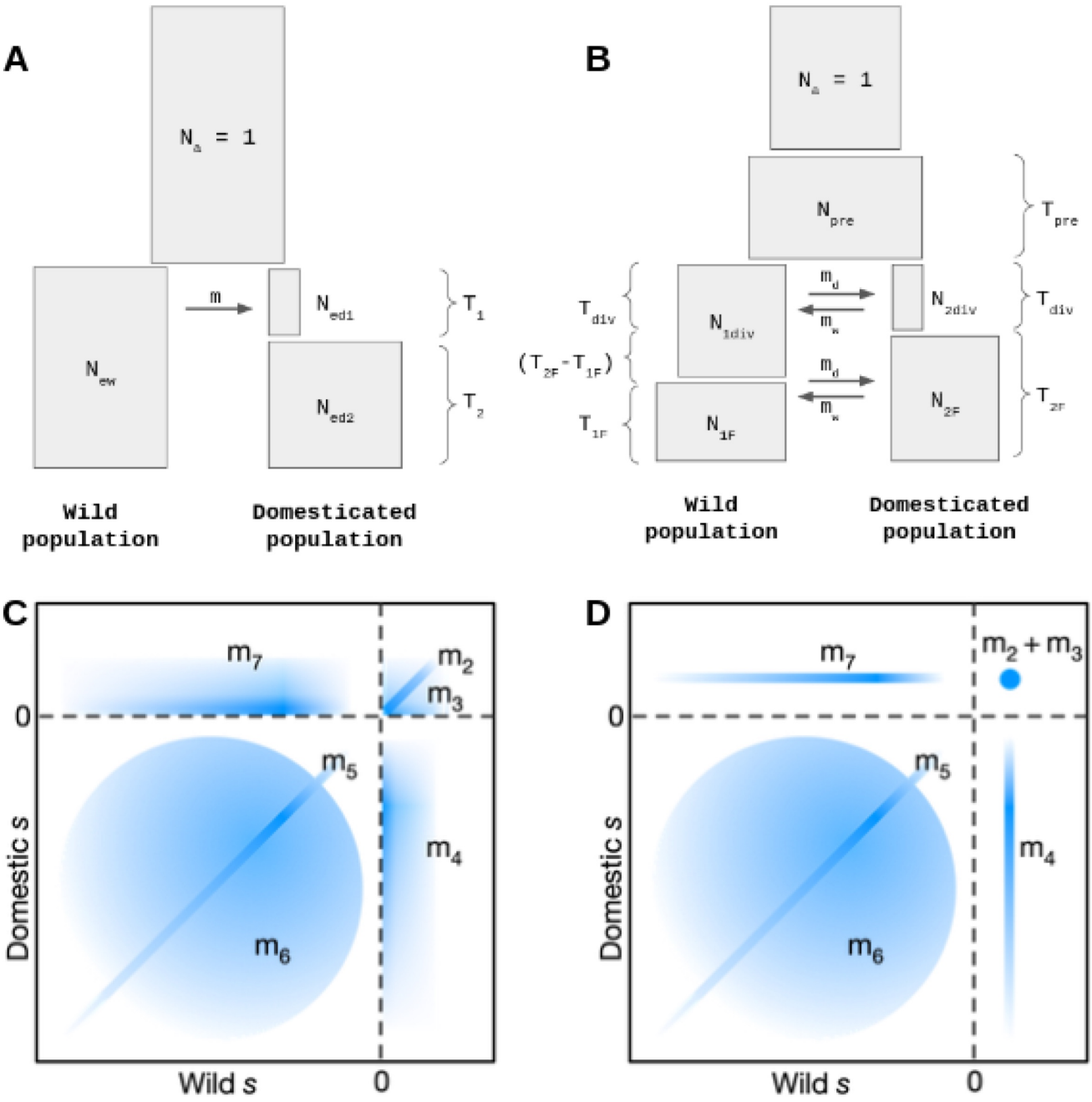
A
N_a = 1
m
N_ew
N_ed1
N_ed2
T_1
T_2
Wild population
Domesticated population
B
N_a = 1
N_pre
T_pre
T_div
(T_2F - T_1F)
T_1F
N_1div
N_2div
N_1F
N_2F
m_d
m_w
T_2F
Wild population
Domesticated population
C
m_7
m_2
m_3
m_5
m_4
m_6
0
Domestic s
Wild s
0
D
m_7
m_2 + m_3
m_5
m_4
m_6
0
Domestic s
Wild s
0

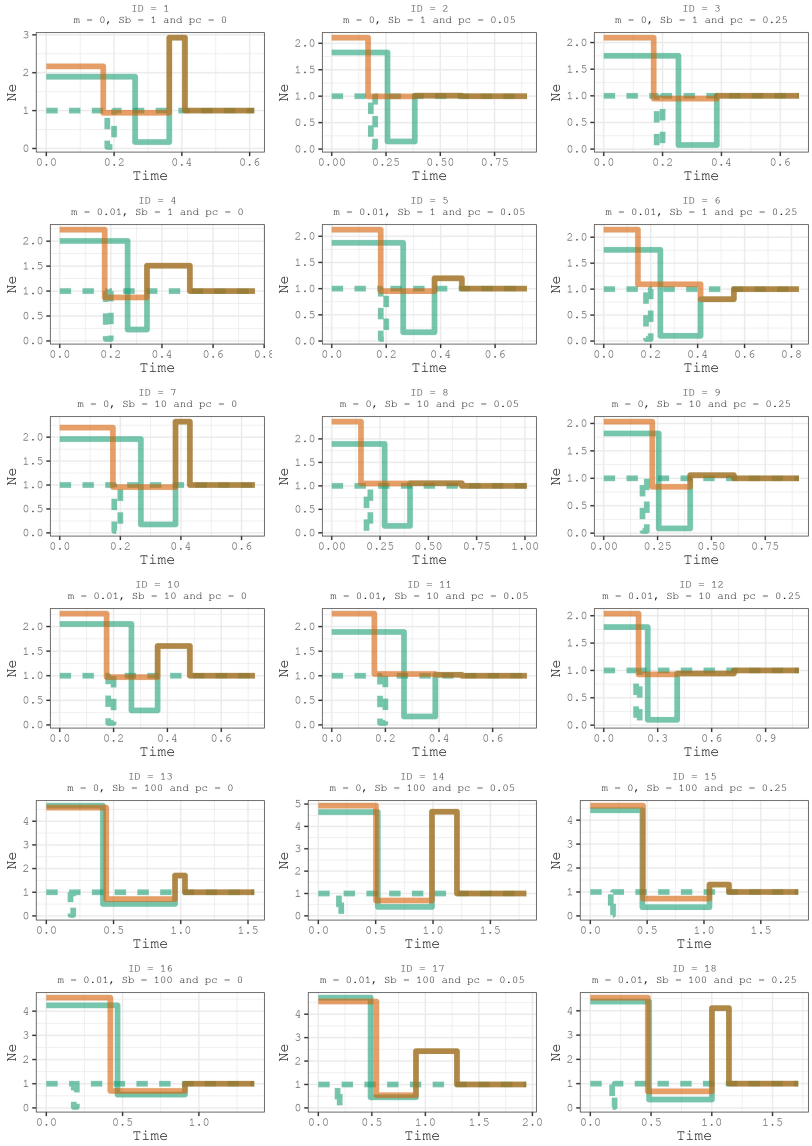
ID = 1
m = 0, Sb = 1 and pc = 0
ID = 2
m = 0, Sb = 1 and pc = 0.05
ID = 3
m = 0, Sb = 1 and pc = 0.25
ID = 4
m = 0.01, Sb = 1 and pc = 0
ID = 5
m = 0.01, Sb = 1 and pc = 0.05
ID = 6
m = 0.01, Sb = 1 and pc = 0.25
ID = 7
m = 0, Sb = 10 and pc = 0
ID = 8
m = 0, Sb = 10 and pc = 0.05
ID = 9
m = 0, Sb = 10 and pc = 0.25
ID = 10
m = 0.01, Sb = 10 and pc = 0
ID = 11
m = 0.01, Sb = 10 and pc = 0.05
ID = 12
m = 0.01, Sb = 10 and pc = 0.25
ID = 13
m = 0, Sb = 100 and pc = 0
ID = 14
m = 0, Sb = 100 and pc = 0.05
ID = 15
m = 0, Sb = 100 and pc = 0.25
ID = 16
m = 0.01, Sb = 100 and pc = 0
ID = 17
m = 0.01, Sb = 100 and pc = 0.05
ID = 18
m = 0.01, Sb = 100 and pc = 0.25
Ne
Time

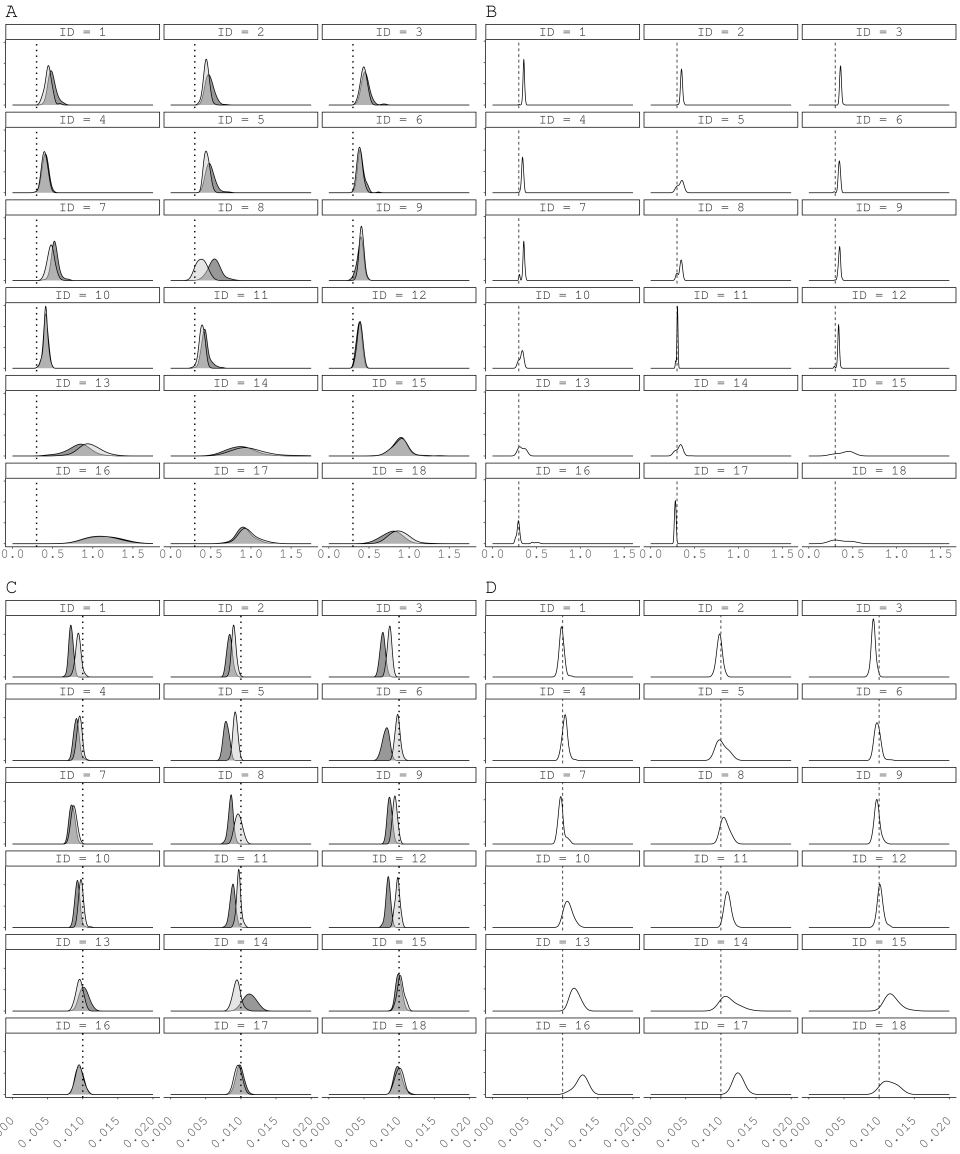
A
B
C
D
ID = 1
ID = 2
ID = 3
ID = 4
ID = 5
ID = 6
ID = 7
ID = 8
ID = 9
ID = 10
ID = 11
ID = 12
ID = 13
ID = 14
ID = 15
ID = 16
ID = 17
ID = 18
0.0 0.5 1.0 1.5
0.000 0.005 0.010 0.015 0.020

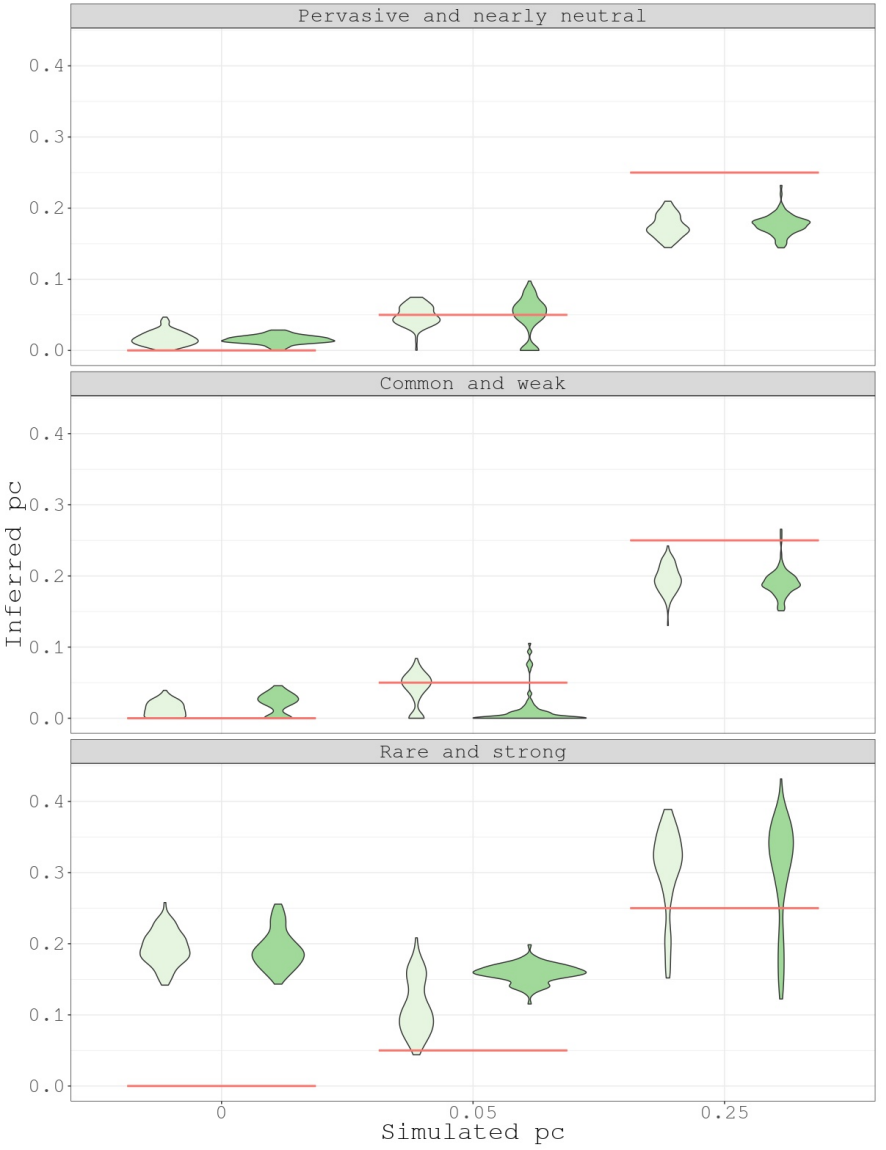
Pervasive and nearly neutral
Common and weak
Rare and strong
Inferred pc
Simulated pc
0.0
0.1
0.2
0.3
0.4
0
0.05
0.25